Title
An empirical approach to retrieving monthly evapotranspiration over Amazonia

Journal
International Journal of Remote Sensing, 29(24)

ISSN
0143-1161

Authors
Juárez, Negrón RI
Goulden, ML
Myneni, RB
et al.

Publication Date
2008-12-01

DOI
10.1080/01431160802226026

International Journal of Remote Sensing
Vol. 29, No. 24, 20 December 2008, 7045–7063

An empirical approach to retrieving monthly evapotranspiration over Amazonia

R. I. NEGRÓN JUÁREZ*†, M. L. GOULDEN‡, R. B. MYNENI§, R. FU†, S. BERNARDES¶ and H. GAO†

†School of Earth and Atmospheric Sciences, Georgia Institute of Technology, Atlanta, GA, USA

‡Earth System Science and Ecology and Evolutionary Biology, University of California, Irvine, CA, USA

§Department of Geography, Boston University, Boston, MA, USA

¶Department of Geography, University of Georgia, Athens, GA, USA

(*Received 30 April 2007; in final form 18 April 2008*)

The extent of evapotranspiration (E_T) over the Brazilian Amazon rainforest remains uncertain because *in situ* measurement sites do not cover the entire domain, and the fetch of these sites is only of the order of 10^3 m. In this investigation we developed an empirical method to estimate E_T over the Brazilian Legal Amazon (BLA). The work was based on an improved physical understanding of what controls E_T over the Amazonia rainforest resulting from analyses of recent *in situ* observations. Satellite data used in this study include the Enhanced Vegetation Index (EVI) from the Moderate Resolution Imaging Spectroradiometer (MODIS) and the surface radiation budget from the International Satellite Cloud Climatology Project (ISCCP). The empirical model was validated by measurements performed at four upland forest sites. The observed values and the calculated modelled values at these sites had the same mean and variance. On a seasonal scale, regional modelled E_T peaks during the austral spring (September to November), as reported in the literature. In addition, the empirical model allows us to estimate the regional seasonal and interannual distributions of E_T/precipitation rates.

1. Introduction

Evapotranspiration (E_T) is a key component that links climate to the terrestrial ecosystem. At specific sites over the Amazon forest, E_T contributes to about 50% of the total precipitation, as calculated by water balance methods and eddy correlation measurements (Salati 1987, Shuttleworth 1988). The geographical variation of this rate remains unknown. Results from the Anglo-Brazilian Amazonian Climate Observation Study (ABRACOS; Gash *et al.* 1996) and the more recent Large-Scale Biosphere-Atmosphere Experiment in Amazonia (LBA) (LBA 1996, Avissar *et al.* 2002, Keller *et al.* 2004) have provided a better understanding of the controls of forest E_T at seasonal and interannual time scales. These studies have shown not only a higher E_T in the dry season than in the wet season but also a higher E_T over areas with less rainfall during the dry season in eastern and central Amazonia (Shuttleworth 1988, Nepstad *et al.* 1994, Malhi *et al.* 2002, Sommer *et al.* 2002,

*Corresponding author. Email: rjuarez@tulane.edu

International Journal of Remote Sensing
ISSN 0143-1161 print/ISSN 1366-5901 online
http://www.tandf.co.uk/journals
DOI: 10.1080/01431160802226026

Souza Filho *et al*. 2005, Negrón Juárez *et al*. 2007). The maintenance of such a high rate of E_T by the rainforest during the dry season plays a central role in determining when the subsequent wet season onset will occur (Fu and Li 2004, Li and Fu 2004). A higher E_T, as a result of the forests responding to increased solar radiation, can also mitigate the impact of moderately dry anomalies on the surface climate condition (Negrón Juárez *et al*. 2007). Therefore, estimation of basin-wide E_T at seasonal to interannual scales is essential for determining seasonal and interannual climate variability in the Amazonian region.

Current techniques used to estimate E_T (e.g. the eddy correlation technique) are limited to point measurements that represent E_T within an area with a radius only of the order of 10^2 to 10^3 m, and as long as the surface characteristics are the same. However, heterogeneities in land surface and soil characteristics mean that extrapolation of point data beyond this area would be inaccurate because of the dynamic and regional variability of E_T. In more remote areas, such as the western Amazon forests, E_T estimates from numerical models (Potter *et al*. 2001) are limited by subjective assumptions that are yet to be validated. Satellite data offer an alternative for estimation of E_T over large areas by complementing previously observed measurements and numerical simulations of E_T. A common approach is to relate E_T to remotely sensed surface temperature (Jackson *et al*. 1977, Hatfield 1983, Jackson 1988, Moran *et al*. 1989, Kustas 1990), solar irradiance (Jackson *et al*. 1983), vegetation indexes (Di Bella *et al*. 2000, Nishida *et al*. 2003*a*,*b*, Loukas *et al*. 2005, Nagler *et al*. 2005, Su *et al*. 2005) or energy balance (Blad and Rosenberg 1974, Bastiaanssen *et al*. 2005) by physical and statistical/semiempirical methods or the Penman–Monteith equation (PM; Monteith 1973, 1981).

Although these methods aim to provide the best possible estimate of E_T, their application to Amazon forests remains unknown because of the lack or inadequacy of meteorological variables required. For instance, calculation of stomatal conductance, an input in the PM equation, is frequently based on the work of Jarvis (1976), but in this case, the main weakness is the assumption that environmental constraints operate independently (Monteith 1995). In addition, values of stomatal conductance at different time scales are not easily comparable, as discussed by the American Society of Civil Engineers (ASCE) Evapotranspiration in Irrigation and Hydrology Committee (Itenfisu *et al*. 2000, Walter *et al*. 2000). Although temperature can be used to estimate E_T over some areas in the Amazon, the relationship between surface temperature and E_T varies in sign across Amazonia. In central-eastern Amazonia, the E_T is in phase with temperature (da Rocha *et al*. 2004, Hutyra *et al*. 2005), while it is out of phase in eastern Amazonia (Sommer *et al*. 2002). E_T is also out of phase with temperature during the wet season over southern Amazonia (Vourlitis *et al*. 2002). These observational results clearly suggest that a simple relationship between surface temperature and E_T does not exist at the basin scale.

Most of the flux tower observations over Amazonian forests during the past two decades have suggested that E_T is primarily controlled by surface radiation and vegetation condition, consistent with that originally reported by Shuttleworth (1988). More recently, Yang *et al*. (2006) have shown that the Enhanced Vegetation Index (EVI; Justice *et al*. 1998, Huete *et al*. 2002) is the most important driver for estimating E_T at a continental scale. Compared to the Normalized Difference Vegetation Index (NDVI), the EVI can better capture canopy structural variation, seasonal vegetation variation, land cover variation, and biophysical variation for high biomass vegetation such as that in Amazonia (Gao *et al*. 2000, Huete *et al*. 2002). The EVI also performs

well under heavy aerosol and biomass burning conditions, which are frequent in the region (Miura *et al.* 1998). The aim of this work was to develop an empirical approach for the estimation of E_T based on the vegetation condition inferred from the EVI and surface net radiation from the International Satellite Cloud Climatology Project (ISCCP; Zhang *et al.* 1995, 2004). The empirical model was trained and validated using data collected at eight upland forest sites over the Brazilian Legal Amazon (BLA).

2. Methodology

2.1 *Study area and model construction*

The study area encompassed the nine states of the BLA (figure 1) covering about 5×10^6 km^2 (Brazilian Institute of Geography and Statistics, www.ibge.gov.br). Latent heat flux (λ_E) data from eight upland sites (table 1) from the LBA experiment were used for model construction and validation. Data from the K83 and RJA sites were used for training the empirical model, and data from the K67 and K34 sites were used for model validation. Other sites (CRS, DCK, SIN and BRG) were used for model comparison.

Observed data show that λ_E has a strong linear relationship with measurements of net radiation (R_n) but at different rates from site to site. For example, figure 2 shows the relationship between daily λ_E and R_n at sites K34, K83 and RJA. Latent heat flux represented ~70% of R_n at K34 and K83, but only 40% at the RJA site, indicating that, for the Amazonia, most of R_n is used to sustain E_T. It is worth noting that vapour pressure deficit (VPD) and wind speed can also influence E_T (Shuttleworth 1988, da Rocha *et al.* 2004, Negrón Juárez *et al.* 2007).

Our empirical model was based on the assumption that E_T over the Amazonian rainforests is primarily a function of EVI and R_n:

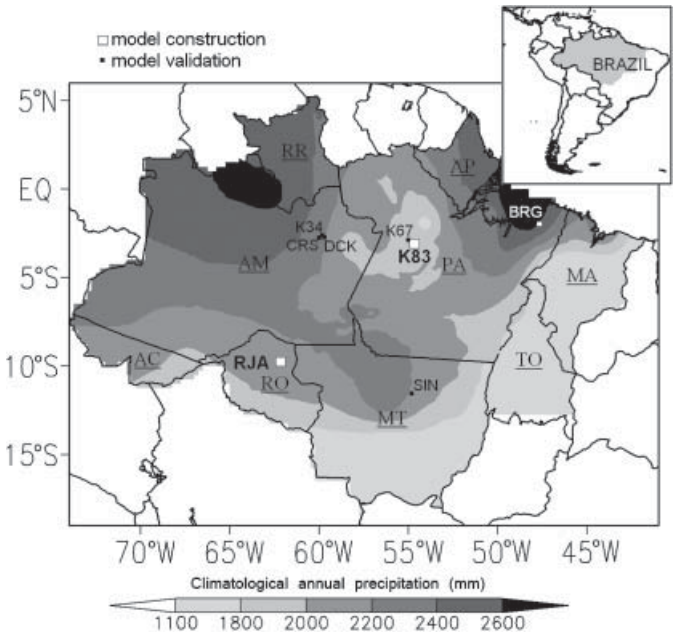

Figure 1. Study area and sites used. The background is the climatological (1961–1990) annual precipitation (mm) over the Brazilian Legal Amazon. For description of sites used see table 1. The states are: AC, Acre; AM, Amazonas; AP, Amapá; MA, Maranhão; MT, Mato Grosso; PA, Pará; RO, Rondônia; RR, Roraima; TO, Tocantins.

Table 1. Sites used in this study.

Site		South latitude (°)	West longitude (°)	Dry season	Method	Source (period of study)
Bragantina* (Igarapé-Açu, Belém, Pará)	BRG	1.1850	47.5706	Sep–Dec	EB	Sommer *et al.* (2002) (Apr 97–Mar 98)
Cuieiras Reserve (Manaus, Amazonas)	CRS	2.5894	60.1153	Jun–Aug	EC	Malhi *et al.* (2002) (Sep 95–Aug 96)
Cuieiras Reserve (Manaus, Amazonas)	K34	2.6090	60.2093	Jun–Aug	EC	Araújo *et al.* (2002)† (Jul 99–Sep 00)
Ducke Reserve (Manaus, Amazonas)	DCK	2.9500	59.9500	Jun–Aug	PM	Shuttleworth (1988) (Sep 83–Sep 85)
Tapajós National Forest (Santarém, Pará)	K67	2.8853	54.9205	Jul–Dec	EC	Hutyra *et al.* (2007)‡ (Jan 02–Jan 06)
Tapajós National Forest (Santarém, Pará)	K83	3.0502	54.9280	Jul–Dec	EC	da Rocha *et al.* (2004)§ (Jul 00–Dec 02)
Biological Reserve of Jarú (Jí-Paraná, Rondônia)	RJA	10.0784	61.9337	Jun–Aug	EC	von Randow *et al.* (2004)† Negrón Juárez *et al.* (2007)‡ (Jan 00–Dec 02)
Sinop¶ (Sinop, Mato Grosso)	SIN	11.4125	55.3250	Jun–Sep	EC	Vourlitis *et al.* (2002) (Aug 99–Jul 00)

EB, energy balance; EC, eddy covariance; PM, Penman–Monteith.
*Secondary vegetation: its height changed from h=2.3 (Apr 97) to h=3.5 m (Mar 98).
†Data available at http://beija-flor.ornl.gov/lba/.
‡Data available at ftp://ftp.as.harvard.edu/pub/tapajos/k67_flux/.
§Data available at http://www.ess.uci.edu/%7Elba/.
¶Transitional (ecotonal) tropical forest.

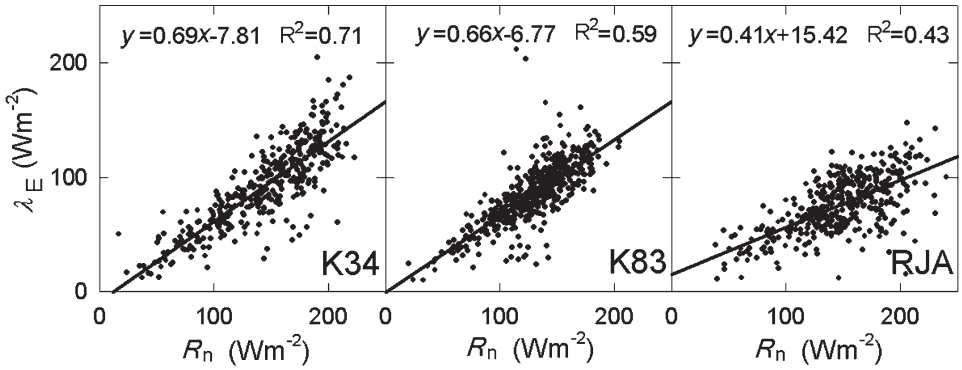

Figure 2. Relationship between net radiation, R_n ($W\,m^{-2}$), and the latent heat flux, λ_E, ($W\,m^{-2}$) at sites K34, K83 and RJA.

$$E_T = f(R_n, E_{VI}) \tag{1}$$

where E_{VI} is the EVI obtained from Moderate Resolution Imaging Spectroradiometer (MODIS) data. The theoretical basis that justifies our model is composed of two factors. First, EVI has been shown to be highly correlated to canopy level CO_2 uptake (Huete *et al*. 2006), and this uptake is closely related to canopy conductance, g_c (Dickinson *et al*. 1991, Sellers *et al*. 1996). Based on physical principles, E_T and g_c are also highly correlated (Monteith 1973, 1981). Therefore, in combination, EVI and E_T should be closely related across sites. Second, R_n is related to E_T (figure 2) through physiological (mainly photosynthesis) and physical processes. Additionally, research has shown that greater R_n increases leaf temperature, which, in turn, drives up the VPD.

Different functions were tested independently at each site. The model that best represented the observed E_T at all sites (E_{T_site}, measured in $mm\,day^{-1}$) was

$$E_{T\_site} = C_1 + C_2 \times E_{VI}^{C3} \times (R_{nISCCP} - C_4) \tag{2}$$

where R_{nISCCP} (measured in Wm^{-2}) is the net radiation from the ISCCP (see section 2.3 for details) and C_1, C_2, C_3 and C_4 are constants.

The percentage error between observed and calculated E_T was calculated as

$$\text{Error} = \pm\left(\frac{1}{n}\sum_{i}^{n}\frac{|Y(i) - Y'(i)|}{Y(i)} \times 100 + \sigma\right) \tag{3}$$

where Y and Y' are the observed and calculated E_T values, respectively, n is the number of elements in the series, and σ is the standard deviation of errors. Constants at K83 and RJA were adjusted to obtain the maximum determination coefficient (R^2) between observed E_T (E_{T_obs}) and modelled E_T (E_{T_grl}) at these sites simultaneously. E_{T_grl} was then used to calculate E_T for the whole BLA.

2.2 *MODIS EVI*

The MODIS EVI products (http://edcdaac.usgs.gov/main.asp) are derived from surface reflectance from the MODIS/Terra sensor, corrected for molecular scattering, ozone absorption and aerosols (Miura *et al.* 2001, Vermote *et al.*

2002). The EVI is designed to optimize signals from vegetation and is sensitive in high biomass regions (Justice *et al.* 1998). The MODIS EVI (E_{VI}) was calculated from the red, near-infrared and blue reflectances (ρ_{red}, ρ_{NIR} and ρ_{blue}, respectively) as:

$$E_{VI} = G(\rho_{NIR} - \rho_{red})/(\rho_{NIR} + a\rho_{red} - b\rho_{blue} + L) \quad (4)$$

The coefficients used in the algorithm are $L=1$, $a=6$, $b=7.5$ and $G=2.5$, with a and b representing the aerosol resistance. Equation (4) uses the blue band to correct the aerosol influence in the red band similar to the Atmosphere Resistant Vegetation Index (ARVI; Kaufman and Tanré 1992). The soil correction coefficient, L, is derived from the Soil-Adjusted Vegetation Index (SAVI; Huete 1988).

Sixteen-day MODIS EVI images with resolution of 1 km (http://modis-land.gsfc.nasa.gov/) from 2000 to 2006 were processed. Monthly data were obtained by using the number of 16-day average images that overlap the calendar month weighted by the number of actual days that overlap that month. The time series of monthly images were then smoothed on a pixel-per-pixel basis using a three-point central-moving-average. For regional estimation, the 1 km resolution data were aggregated to 0.25°. For model construction and validation, a three-pixel box centred in the tower location was used. Figure 3 shows the monthly EVI at the K67, K83, K34 and RJA sites at 1 km and 0.25° resolutions for the period 2000–2004. It was verified that EVI values after aggregation had the same mean (*t*-Student, not shown) and variance (*F*-test, not shown).

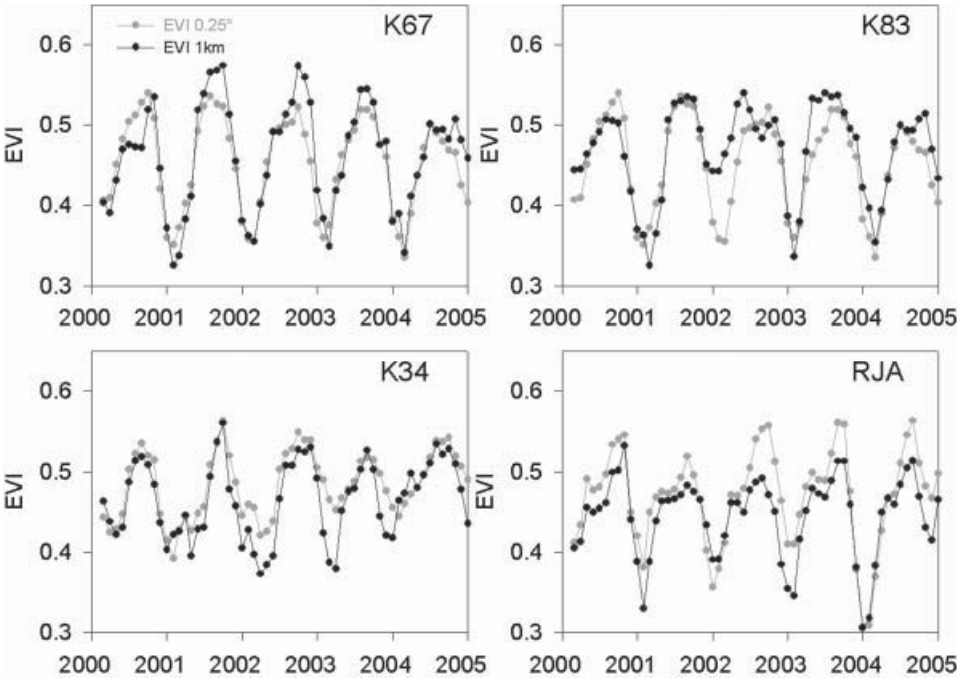

Figure 3. Comparison of monthly EVI time series at 1 km and 0.25° horizontal resolution at K67, K83, K34 and RJA sites for the period 2000–2004.

2.3 *ISCCP R_n data*

Monthly net surface radiation (R_{nISCCP}) was calculated for the period from July 1983 to December 2004, at a spatial resolution of 2.5°. The calculation was based on surface balance of shortwave (0.2–5.0 μm) and longwave (5.0–200 μm) radiative flux data at full-sky conditions from the ISCCP. Full-sky fluxes were weighted from fluxes calculated for 15 types of cloudy conditions and clear-sky fluxes by their fractional coverage for each cell. Zhang *et al*. (1995, 2004) have presented a complete description of this data set.

For model construction and validation, we used the R_{nISCCP} encompassing the tower coordinates. For the regional estimation of E_{T}, the R_{nISCCP} data were interpolated to a spatial resolution of 0.25° using the Kriging interpolation method (Oliver and Webster 1990). Figure 4 shows that R_{nISCCP} at 0.25° and at 2.5° agree fairly well; however, an offset was observed when compared to the observed R_{n}. The *F*-test statistics (and its probability) between observed R_{n} and R_{nISCCP} at 0.25° for the K67, K34, K83 and RJA sites was 1.074 (0.839), 1.569 (0.392), 1.245 (0.559) and 2.667 (0.005), respectively. Except for the RJA site, R_{nISCCP} at 0.25° had the same variance with respect to the observed R_{n}. A detailed analysis of observed R_{n} and R_{nISCCP} at RJA showed that the *F*-statistics for the period from January 2000 to

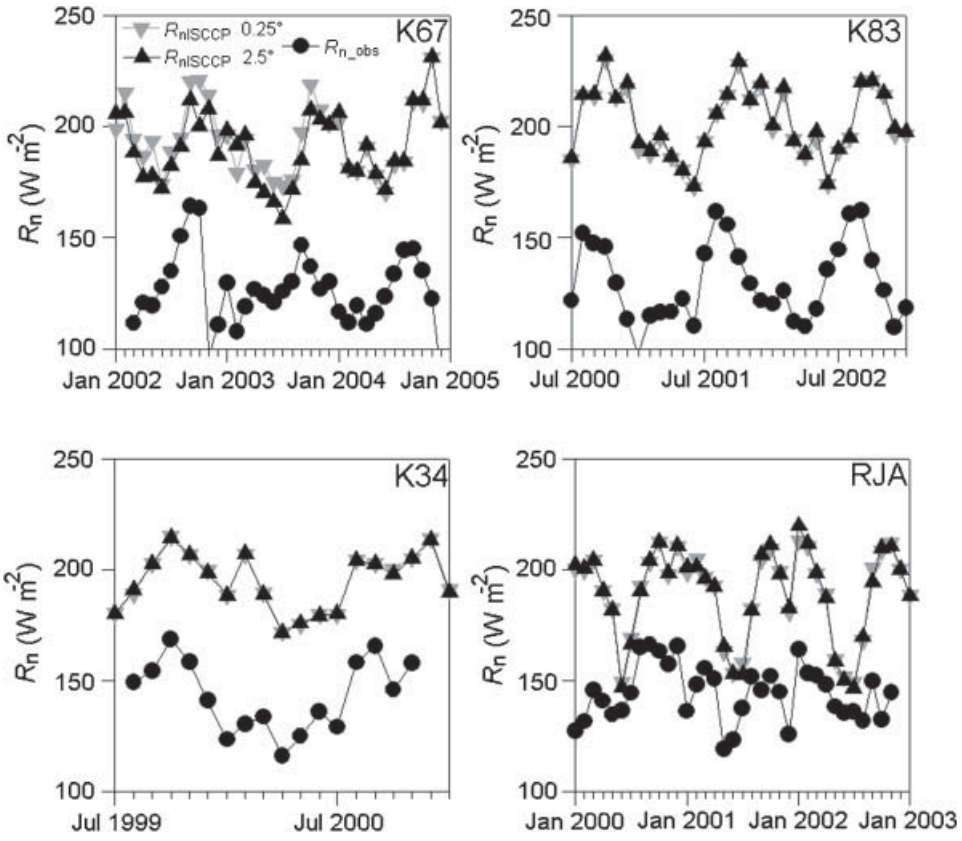

Figure 4. Comparison between observed net radiation, $R_{\mathrm{n\_obs}}$ (W m^{-2}), and net radiation calculated from ISCCP data, R_{nISCCP}, at 2.5° and 0.25° horizontal resolution at K67, K83, K34 and RJA sites.

December 2001 is 1.9, and its probability is 0.133, indicating that the observed and satellite series had the same variance.

3. Results

3.1 *Model training and validation*

Figure 5 shows the observed and calculated E_T at K83, RJA, K67 and K34. The empirical formula trained for best fit at each specific site (E_{T_site}) generally provided a close match with the observed data (E_{T_obs}) at seasonal and interannual scales. However, at the RJA site, E_{T_site} overestimated the annual maximum E_T. The determination coefficients (R^2 at 95% CI, F-test) between E_{T_site} and E_{T_obs} were 0.64 at the K83 site, 0.62 at the K67 site, 0.8 at the K34 site, and 0.32 at the RJA site. The general empirical model (E_{T_grl}) used to calculate the E_T over the BLA was obtained using coefficients $C_1=2.7$, $C_2=0.05$, $C_3=1.75$ and $C_4=140$. The R^2 values (95% CI, F-test) between E_{T_grl} and E_{T_obs} were 0.61, 0.55, 0.8 and 0.31 at the K83, K67, K34 and RJA sites, respectively. The associated errors between E_{T_site} (E_{T_grl}) and E_{T_obs} at these sites were $\pm 17\%$ ($\pm 19\%$), $\pm 11\%$ ($\pm 13\%$), $\pm 6\%$ ($\pm 9\%$), and $\pm 12\%$ ($\pm 20\%$), respectively. Using both R_{nISCCP} and EVI at 0.25° spatial resolution, the E_{T_grl} errors with respect to E_{T_obs} at K67, K83, K34 and RJA were $\pm 18\%$, $\pm 19\%$, $\pm 16\%$ and $\pm 16\%$, respectively, with an average error of $\pm 17\%$. This shows that the 0.25° resolution did not significantly diminish the quality of the calculated E_T.

Figure 6 compares the seasonal mean of E_{T_grl} for the period 2000–2004 at 1 km and 0.25° resolutions with respect to E_{T_obs} for the sites and periods listed in table 1. At the K34, K83, K67 and RJA sites, the average difference between E_{T_obs} and

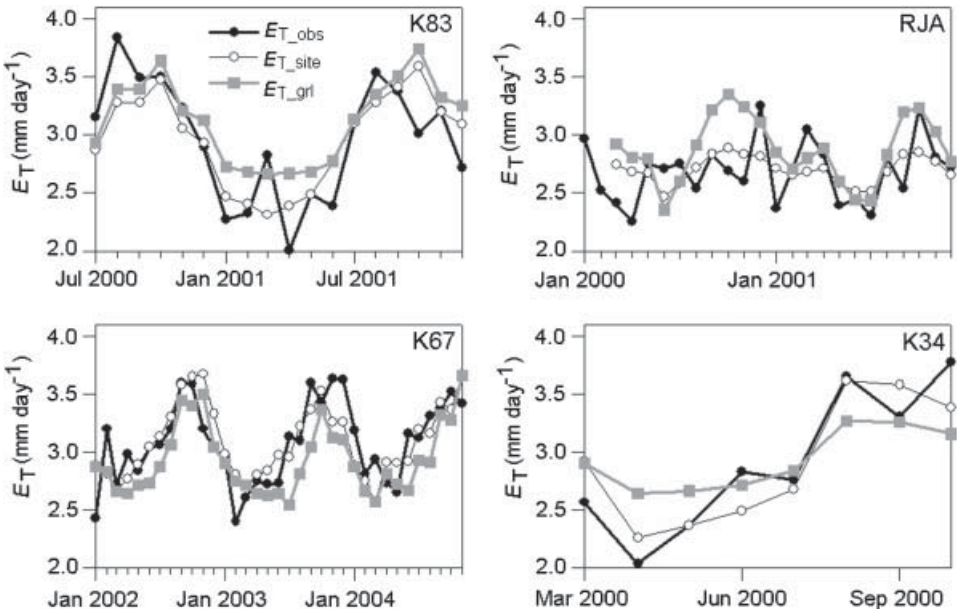

Figure 5. Comparison between observed, E_{T_obs} (solid black line), and calculated values of evapotranspiration using a calibrated model for each site, E_{T_site} (grey line and open circles) and a general model based on K83 and RJA sites, E_{T_grl} (grey line and filled squares), for sites K83, RJA, K67 and K34.

E_{T_grl} at 1 km of horizontal resolution was 8% during the wet season and 10% during the dry season. The differences at 0.25° resolution were very similar to the 1 km data, with a difference during the wet season of 8% and a difference during the dry season of 9%. At the CRS, DCK, BRG and SIN sites, the average difference between E_{T_obs} and E_{T_grl} during the wet season was 26% and 18% at 1 km and 0.25° resolutions, respectively. During the dry season these differences were 18% at 1 km resolution and 19% at 0.25° resolution. The best agreement, approximately 11%, occurs at the CRS site in central equatorial Amazonia, located near the K34 site. The worst agreement, about 30%, is associated with the BRG site, located near the mouth of the Amazon River, where the climate is strongly influenced by wind coming from the ocean. Thus, on seasonal and interannual scales the maximum discrepancy between E_{T_grl} and E_{T_obs} is about 30%, a value that is comparable to the uncertainties of *in situ* measurements of E_T (e.g. see references in table 1).

Several factors can contribute to the discrepancies shown in figure 6. For instance, the satellite inputs associated with surface solar radiation and the EVI may be different from those at the flux towers, in part due to the lack of information on subscale structures within the satellite footprints. The observed values also have significant uncertainties due to instrumental errors, as well as the different methods involved in the calculation of E_T. For instance, the E_T values at the DCK site were obtained from a combination of observed and calculated data using the Penman–Monteith equation, while the BRG site E_T was calculated using both the Bowen ratio energy balance and the Penman–Monteith equation. The reported E_T values at the SIN site were obtained using the eddy correlation system and the Priestley–Taylor model (Priestley and Taylor 1972).

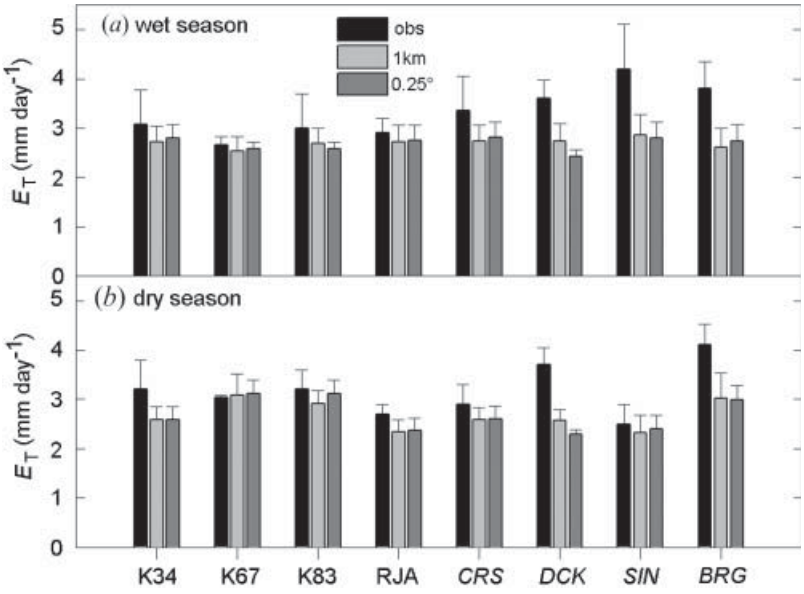

Figure 6. Observed (black bar) and calculated values of evapotranspiration (E_T) at 1 km (light grey bar) and 0.25° (dark grey bar) of horizontal resolution during (*a*) the wet season and (*b*) the dry season. The observed E_T was obtained for periods described in table 1 and the calculated E_T values correspond to the period 2000–2004 (except 2002). Sites in italics indicate that the periods of observed E_T values are out of the estimated period.

3.2 *Seasonal E_T*

Figure 7 shows the average seasonal E_T and precipitation for the period 2000–2004 over BLA. Precipitation data are from the Tropical Rainfall Measuring Mission (TRMM) 3B43 product (http://trmm.gsfc.nasa.gov), which uses TRMM data merged with other satellite data and available rain gauge records. This dataset has proven to be consistent with rain gauge data (Negrón Juárez *et al*. 2007) and has the advantage of a high spatial resolution. From December to February (DJF), the maximum values of E_T ($\sim$3 mm day^{-1}, figure 7(*a*)) appeared in the north of the Amazonas State, whereas precipitation was higher in southern BLA (>8 mm day^{-1}, figure 7(*b*)). From March to May (MAM), E_T did not have extreme spatial changes over BLA, showing an average value of 2.6 mm day^{-1}, with some areas in Maranhão State having values of 2.9 mm day^{-1}. During this period, precipitation was concentrated over the northern BLA, reaching values higher than 6 mm day^{-1} (lower values were observed over the north of Roraima State, RR in figure 1). The period from June to August (JJA) showed a gradient of precipitation (E_T) from south to north, with values ranging from 3 mm day^{-1} (2 mm day^{-1}) to 7 mm day^{-1} (2.8 mm day^{-1}). Maximum E_T values of about 3 mm day^{-1} were observed in the north of Pará State. From September to November (SON), E_T ranged from 3 to 3.3 mm day^{-1}, except over the Cerrado domain (see figure 11) in the southern BLA, where E_T ranged from 2.2 to 2.5 mm day^{-1}. In the eastern Amazonia E_T was higher than 3.1 mm day^{-1} when precipitation was lower than 3 mm day^{-1}, which is consistent with previous *in situ* observations (Nepstad *et al*. 1994, da Rocha *et al*. 2004, Oliveira *et al*. 2005). The increase of E_T in eastern Amazonia from September to November is consistent with higher values of EVI and R_n, as observed by Huete *et al*. (2006). However, the adjacent deforested areas presented lower values of E_T as well as of the EVI during the dry season, as reported in other studies (Huete *et al*. 2006, Myneni *et al*. 2007).

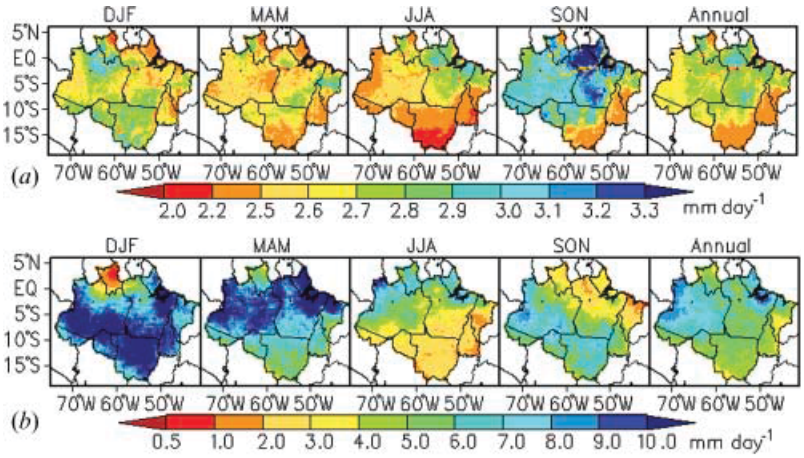

Figure 7. Three-month average values (DJF, MAM, JJA, SON) and annual average values of (*a*) calculated E_T (mm day^{-1}) and (*b*) precipitation (mm day^{-1}), over the Brazilian Legal Amazon. Values were calculated for the period 2000–2004. Precipitation corresponds to the TRMM 3B43 data sets.

4. Discussion

4.1 *Sensitivity of EVI to climate variability*

In this paper, EVI is used to represent changes in vegetation, including the response of vegetation to climate variability. It is important to ask how adequate EVI is in representing the geographic seasonal to interannual variation of vegetation. The Amazon forest is dominated by its response to rainfall variation on these time scales. The capability of EVI to monitor the seasonal variation of the Amazon forest was studied by Xiao *et al.* (2006). To study the capability of EVI to monitor the interannual variability of Amazon forest we performed an analysis over an area in the eastern Amazon (2° S–5° S, 53° W–56° W) that experiences regular droughts from El Niño events (Stokstad 2005). In this area, the dry season lasts 5 months (consecutive months with precipitation <100 mm) centred in September (Sombroek 2001). Droughts are one of the most important climate variability events in the Amazon, having a strong influence over vegetation phenology. We diagnose these events using the Standardized Precipitation Index (SPI; McKee *et al.* 1993), calculated for the period 1986–2006, and based on precipitation data from the Global Precipitation Climatological Centre (GPCC). The SPI value is equal to zero if precipitation does not deviate from its climatology. Droughts begin when SPI values first fall below zero and end with positive or zero values of SPI for at least several months.

Figure 8(*a*) shows monthly SPI time series from 2000 to 2006. During this period, drought events with different intensities can be observed in 2002, 2003 and 2005. The 2002–2003 drought, but not the 2005 drought, can be related to an El Niño event (McPhaden 2004, Marengo *et al.* 2008). It can also be observed that, except for some months during the dry season, the precipitation in 2002 was below its long-term average, with a deficit starting around July 2001. Coincident with this deficit, figure 8(*b*) shows that, during the 2002 dry season, the EVI had the lowest values among the drought events compared. This result agrees with Hutyra *et al.* (2007), who reported that the gross primary productivity for the period 2002–2005 was lower during the 2002 dry season in the K67 site. As EVI is sensitive to canopy

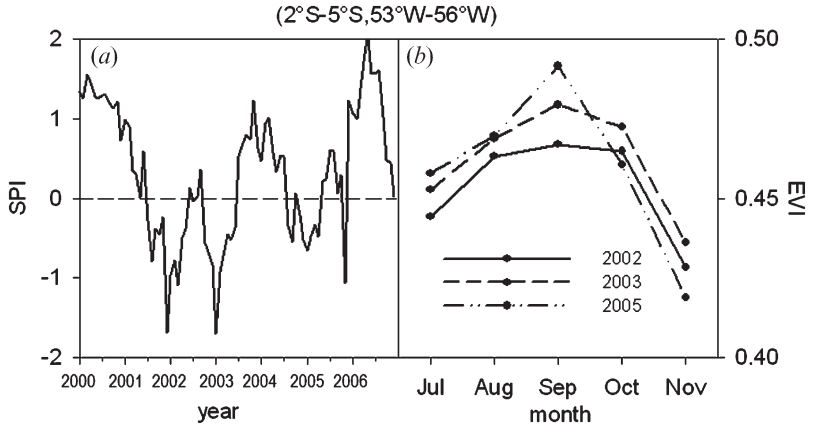

Figure 8. Monthly spatial average values over the area 2° S–5° S and 53° W–56° W of (*a*) the Standardized Precipitation Index (SPI) from 2000 to 2006 and (*b*) the dry season EVI from 2002 to 2005. The SPI was calculated from the GPCC data (1986–2006) using a time scale of 6 months.

structure, low EVI values can be associated with a thinning of the leaf canopy or canopy openness as a consequence of drought conditions, as reported for this region by Nepstad *et al*. (2002). In 2003, above average precipitation started in July and continued throughout July 2004. The increase of precipitation during the 2003 dry season produced a favourable effect on vegetation (an increase in EVI values) with respect to the same period in 2002. In 2005, South America experienced below-normal precipitation anomalies, but in west-central and eastern Brazil the rainy season was slightly below normal (Shein 2006). In this year, after 6 months of wetter than normal precipitation conditions, a moderate drought event was observed in September. The EVI shows a peak in this month due to the positive response of vegetation to well-watered soil and an increase in solar radiation.

Although vegetation green-up has been reported during the dry season in the eastern Amazon (Huete *et al*. 2002), our results show that the intensity of this green-up depends strongly on climate variability. The EVI was capable of monitoring forest conditions related to this variability.

4.2 *Uncertainties of observed and calculated E_T*

First, *in situ* measurements of E_T have uncertainties of about 10–30%, as suggested by the observed imbalance of 14% (K83) to 28% (RJA) (see table 1 for references), related to several factors (e.g. advection, night flux underestimations).

Second, cloud cover can reduce the quality of MODIS EVI data. Asner (2001) reported that the chance of acquiring scenes with 30% or less cloud cover over the Amazon is minimal from December to May and very limited from October to November. Annually, the probability of obtaining scenes with 30% or less cloud cover in the BLA is >90% southwards of 5° S. The MODIS science team established the Vegetation Index Usefulness Index (UI; http://edcdaac.usgs.gov/modis/moyd13_qa_v4.asp) as a quality assessment on a pixel-by-pixel basis. We used the UI to evaluate the quality of the EVI images. The values of the UI for a pixel are determined by several factors, including aerosol quantity, atmospheric correction conditions, cloud cover, shadow, and sun-target-viewing geometry. The UI has 16 levels that vary from perfect quality (level 0) to low quality (level 14). No useful data are labelled as level 15. In this work the level 'Intermediate Quality' (sixth in the UI scale) was used as the threshold between good and bad quality pixels. This threshold is more restrictive than the 'Average Quality' (eighth in the UI scale) commonly used.

The 16-day 1 km × 1 km usefulness quality data were used to calculate the percentage of pixels with quality better than the 'Intermediate Quality' level. The results were then converted to 0.25° resolution and are presented in figure 9. Central Pará had good quality EVI in 30–40% of images. This percentage was higher, near 50%, over western Maranhão, southern Amapá, some areas in Roraima, and the western portion of Amazonas State. The remaining areas presented EVI better than the threshold in at least 60% of the cases, with the best EVI quality being observed in the southern and western edges of the BLA. Our model represented the observations at central Pará (K83 and K67 sites) well, overcoming the effects of pixel quality. However, on the western edge of BLA, the E_T values should be considered with caution because observed E_T data are not available for comparison.

A third factor contributing to errors in E_T are uncertainties in ISCCP-FD fluxes. The largest sources of uncertainties for South America are caused by clouds, TIROS Operational Vertical Sounder (TOVS) atmospheric temperature, ISCCP surface

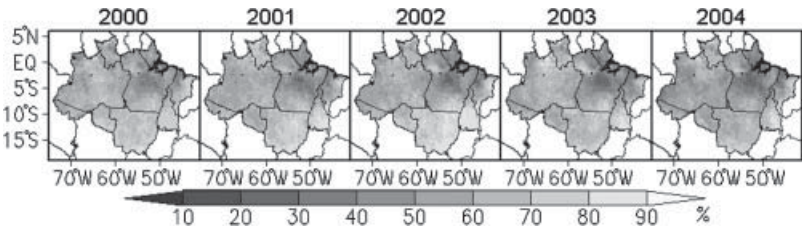

Figure 9. Areas in the Brazilian Legal Amazon with recurrent problems of MODIS EVI quality. The grey-scale indicates the frequency that pixels have better than 'Intermediate Quality' over the course of a year.

temperatures, and vertical water vapour profiles (Zhang *et al*. 2004). Zhang *et al*. (2004) reported that the overall uncertainties of these fluxes are at least 10–15 W m^{-2} at the surface. Although the differences between the site observations and the ISCCP-FD fluxes presented here are larger than that, the differences appears to be constant throughout the BLA (figure 4), presumably because of differences in spatial and temporal scales between satellite and flux tower measurement footprints.

4.3 *E_T/precipitation rates over the Amazon*

The rate of E_T determined with respect to precipitation across the Amazon forest is shown in figure 10. The DCK, CRS, K83 and SIN sites reported an average E_T/precipitation rate of 50% and the RJA site had a rate of 45%. Our results agree with these measurements but also show a regional variability in this rate. Areas of maximum precipitation (see also figure 1) had the lowest rate (<40%). These areas also show from zero to three consecutive months with precipitation <100 mm and lower daylight intensity (Sombroek 2001). High precipitation implies high cloudiness, and therefore less radiation available to promote E_T. These areas also have the maximum plant-available soil water (PAW) and are less susceptible to droughts than those observed during an El Niño event (Nepstad *et al*. 2004). E_T/precipitation rates with values greater than 40% were observed in southern, eastern and middle areas of the basin. These areas are characterized by annual precipitation <2000 mm (figure 1), 4–7 consecutive months of precipitation <100 mm (Sombroek 2001) and low values of maximum PAW (Nepstad *et al*. 2004), and their temperatures strongly correlated with

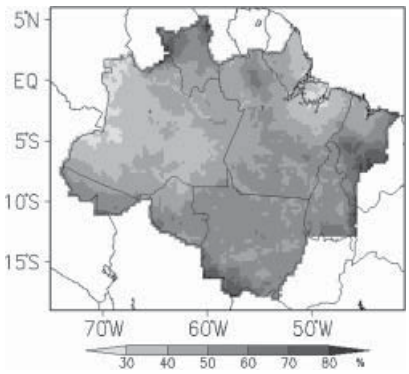

Figure 10. Percentage of evapotranspiration with respect to precipitation over the Brazilian Legal Amazon for the period 2000–2004.

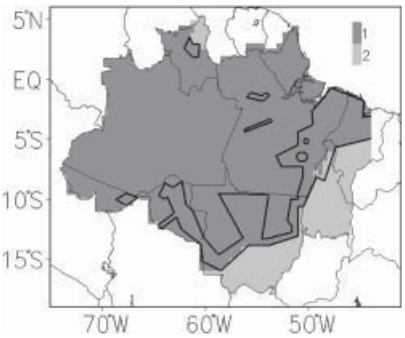

Figure 11. Distribution of forest (1) and savanna (2) across the Brazilian Legal Amazon. Area inside the solid line roughly represents areas with strong deforestation (source: www.obt.inpe.br/prodes/).

the El Niño-Southern Oscillation (ENSO) index (Malhi and Wright 2004). As a result, these areas are more susceptible to drought events and fires.

4.4 *E_T over deforested areas*

Since the early 1970s, the Amazon basin has been heavily deforested in an area along the southern and eastern edges of the basin, as delineated in figure 11. By August 2004 the accumulated deforestation was ~14% of the BLA (www.obt.inpe.br/prodes). After 2002, an increase in the deforestation rate was observed in response to the increased international demand for soybeans (especially in the state of Mato Grosso) and beef (Fearnside 2005). To determine whether calculated E_T is adequate over deforested areas we focused our analysis over a small area within the coordinates 10° S to 11° S and 55° W to 56° W in the Mato Grosso State, where intense deforestation has occurred in recent years. During the wet and dry season our model shows E_T values of 2.8 ± 0.13 and 2.2 ± 0.1 mm day^{-1}, respectively. These values are very close to those of 3.2 mm day^{-1} in December and 2.12 mm day^{-1} for the dry season reported by Priante *et al.* (2004) over a cattle pasture area located at 9.86° S and 55.23° W in the Mato Grosso State. These results suggest that our model may be used as a first approximation of E_T over deforested areas.

5. Conclusions

The empirical model developed to calculate E_T, using satellite-retrieved net radiation and EVI as inputs, agrees with *in situ* observations within 17%. This empirical model was based on the suggestion from previous *in situ* observations that the distribution of E_T over the Amazon is largely controlled by the surface net radiative flux and vegetation condition. Our analysis suggests that the EVI can reasonably capture the vegetation responses due to rainfall variability on a large scale. The rates of E_T/precipitation were very similar to those reported in the literature over the BLA; although MODIS EVI data are reduced in quality over Pará State, the calculated E_T agreed well with observed E_T, with high values over the northern part of this state during the dry season (September to November). Our model enabled us to determine a regional pattern of the E_T. The model also shows a reasonable change in E_T over deforested areas compared to *in situ* observations. However, further studies are needed to more clearly determine whether this method can be used to estimate E_T over areas where change in land cover has occurred.

Acknowledgements

We acknowledge the LBA community for both their extensive field measurements, which provide data focused on the understanding of the Amazon forest, and for making these data available through the LBA Beija-Flor search and retrieval system (http://beija-flor.ornl.gov/lba). We thank Susan Ryan and John Trostel for their valuable editorial assistance. We are also grateful to the constructive comments made by the three anonymous reviewers. This work was supported by the NASA Terrestrial Ecology Program for the Earth System Science Research Using Data and Products from Terra and ACRIM Satellites.

References

Araújo, A.C., Nobre, A.D., Kruijt, B., Elbers, J.A., Dallarosa, R., Stefani, P., Von Randow, C., Manzi, A.O., Culf, A.D., Gash, J.H., Valentini, R. and Kabat, P., 2002, Comparative measurements of carbon dioxide fluxes from two nearby towers in a central Amazonian rainforest: the Manaus LBA site. *Journal of Geophysical Research-Atmospheres*, **107**, 8090, doi:10.1029/2001JD000676.

Asner, G.P., 2001, Cloud cover in Landsat observations of the Brazilian Amazon. *International Journal of Remote Sensing*, **22**, pp. 3855–3862.

Avissar, R., Dias, P.L.S., Dias, M.A.F.S. and Nobre, C., 2002, The Large-Scale Biosphere-Atmosphere Experiment in Amazonia (LBA): insights and future research needs. *Journal of Geophysical Research-Atmospheres*, **107**, 8086, doi:10.1029/2002JD002704.

Bastiaanssen, W.G., Noordman, E.J., Pelgrum, H., Davids, G., Thoreson, B.P. and Allen, R.G., 2005, SEBAL model with remote sensed data to improve water-resources management under actual field conditions. *Journal of Irrigation and Drainage Engineering*, **131**, pp. 85–93.

Bland, B.L. and Rosenberg, N.J., 1974, Lysimetric calibration of the Bowen ratio-energy balance method for evapotranspiration estimation in the Central Great Plains. *Journal of Applied Meteorology*, **13**, pp. 227–236.

da Rocha H.R., Goulden, M.L., Miller, S.D., Menton, M.C., Pinto, L.D.V.O., de Freitas H.C. and Figueira, A.M.E.S., 2004, Seasonality of water and heat fluxes over a tropical forest in eastern Amazonia. *Ecological Applications*, **14**, pp. S22–S32.

Di Bella, C.M., Rebella, C.M. and Paruelo, J.M., 2000, Evapotranspiration estimates using NOAA AVHRR imagery in the Pampa region of Argentina. *International Journal of Remote Sensing*, **21**, pp. 791–797.

Dickinson, R.E., Henderson-Sellers, A., Rosenzweig, C. and Sellers, P.J., 1991, Evapotranspiration models with canopy resistance for use in climate models: a review. *Agricultural and Forest Meteorology*, **54**, pp. 373–388.

Fearnside, P.M., 2005, Deforestation in Brazilian Amazonia: history, rates and consequences. *Conservation Biology*, **19**, pp. 680–688.

Fu, R. and Li, W., 2004, The influence of the land surface on the transition from dry to wet season in Amazonia. *Theoretical and Applied Climatology*, **78**, pp. 97–110.

Gao, X., Huete, A.R., Ni, W. and Miura, T., 2000, Optical–biophysical relationships of vegetation spectra without background contamination. *Remote Sensing of Environment*, **74**, pp. 609–620.

Gash, J.H.C., Nobre, C.A., Roberts, J.M. and Victoria, R.L., 1996, An overview of ABRACOS. In *Amazonian Deforestation and Climate*, J.H.C. Gash, C.A. Nobre, J.M. Roberts and R.L. Victoria (Eds), pp. 1–14 (Chichester: John Wiley & Sons).

Hatfield, J.L., 1983, Evapotranspiration obtained from remote sensing methods. In *Advances in Irrigation*, D.E. Hilled (Ed.), pp. 395–416 (New York: Academic Press).

Huete, A., Didan, K., Miura, T., Rodriguez, E.P., Gao, X. and Ferreira, L.G., 2002, Overview of the radiometric and biophysical performance of the MODIS vegetation indices. *Remote Sensing of Environment*, **83**, pp. 195–213.

HUETE, A.R., 1988, A soil-adjusted vegetation index (SAVI). *Remote Sensing of Environment*, **25**, pp. 295–309.

HUETE, A.R., DIDAN, K., SHIMABUKURO, Y.E., RATANA, P., SALESKA, S.R., HUTYRA, L.R., YANG, W., NEMANI, R. and MYNENI, R., 2006, Amazon rainforest green-up with sunlight in dry season. *Geophysical Research Letters*, **33**, L06405, doi:10.1029/2005GL025583.

HUTYRA, L.R., MUNGER, J.W., SALESKA, S.R., GOTTLIEB, E.W., DAUBE, B.C., DUNN, A.L., AMARAL, D.F., CAMARGO, P.B. and WOFSY, S.C., 2007, Seasonal controls on the exchange of carbon and water in an Amazonian rain forest. *Journal of Geophysical Research-Biogeosciences*, **112**, GO3008, doi: 10.1029/2006JG000365.

HUTYRA, L.R., MUNGER, J.W., NOBRE, C.A., SALESKA, S.R., VIEIRA, S.A. and WOFSY, S.C., 2005, Climatic variability and vegetation vulnerability in Amazonia. *Geophysical Research Letters*, **32**, L24712, doi:10.1029/2005GL024981.

ITENFISU, D., ELLIOTT, R.L., ALLEN, R.G. and WALTER, I.A., 2000, Comparison of reference evapotranspiration calculations across a range of climates. In *Proceedings 4th Decennial National Irrigation Symposium*, R.G. Evans, B.I. Benham and T.P. Trooien (Eds), pp. 216–227 (St Joseph, MI: American Society of Agricultural Engineers).

JACKSON, R.D., REGINATO, R.J. and IDSO, S.B., 1977, Wheat canopy temperature: a practical tool for evaluating water requirements. *Water Resources Research*, **13**, pp. 651–656.

JACKSON, R.D., 1988, Surface temperature and the surface energy balance. In *Flow and Transport in the Nature Environment: Advances and Application*, W.L. Steffen and O.T. Dermard (Eds), pp. 133–153 (Berlin: Springer-Verlag).

JACKSON, R.D., HATFIELD, J.L., REGINATO, R.J., IDSO, S.B. and PINTER, P.J. JR., 1983, Estimation of daily evapotranspiration from one time-of-day-measurements. *Agricultural Water Management*, **7**, pp. 351–362.

JARVIS, P.G., 1976, The interpretation of the variations in leaf water potential and stomatal control conductance found in canopies in the field. *Philosophical Transactions of the Royal Society of London, Series B*, **273**, pp. 593–610.

JUSTICE, C.O., VERMOTE, E., TOWNSHEND, J.R.G., DEFRIES, R., ROY, D.P., HALL, D., SALOMONSON, V., PRIVETTE, J., RIGGS, G., STRAHLER, A., LUCHT, W., MYNENI, R., KNYAZIKHIN, Y., RUNNING, S., NEMANI, R., WAN, Z., HUETE, A., VAN LEEUWEN W., WOLFE, R., GIGLIO, L., MULLER, J., LEWIS, P. and BARNSLEY, M., 1998, The Moderate Resolution Imaging Spectroradiometer (MODIS): land remote sensing for global change research. *IEEE Transactions on Geoscience and Remote Sensing*, **36**, pp. 1228–1248.

KAUFMAN, Y.J. and TANRÉ, D., 1992, Atmospherically resistant vegetation index (ARVI) for EOS-MODIS. *IEEE Transactions on Geoscience and Remote Sensing*, **30**, pp. 261–270.

KELLER, M., ALENCAR, A., ASNER, G.P., BRASWELL, B., BUSTAMANTE, M., DAVIDSON, E., FELDPAUSCH, T., FERNANDES, E., GOULDEN, M., KABAT, P., KRUIJT, B., LUIZAO, F., MILLER, S., MARKEWITZ, D., NOBRE, A.D., NOBRE, C.A., FILHO, N.P., DA ROCHA H., DIAS, P.L.D.S., VON RANDOW, C. and VOURILITIS, G., 2004, Ecological research in the Large-Scale Biosphere-Atmosphere Experiment in Amazonia: early results. *Ecological Applications*, **14**, pp. S3–S16.

KUSTAS, W.P., 1990, Estimates of evapotranspiration with a one- and two-layer model of heat transfer over partial canopy cover. *Journal of Applied Meteorology*, **29**, pp. 704–715.

LBA, 1996, *The Large-Scale Biosphere-Atmosphere Experiment in Amazonia: Concise Experimental Plan*, The LBA Science Planning Group. Document available at CPTEC/INPE, Cachoeira Paulista, SP, Brazil.

LI, W. and FU, R., 2004, Transition of the large-scale atmospheric and land surface conditions from the dry to the wet season over Amazonia as diagnosed by the ECMWF reanalysis. *Journal of Climate*, **17**, pp. 2637–2651.

LOUKAS, A., VASILIADES, L., DOMENIKIOTIS, C. and DALEZIOS, N.R., 2005, Basin-wide actual evapotranspiration estimation using NOAA/AVHRR satellite data. *Physics and Chemistry of the Earth*, **30**, pp. 69–79.

MALHI, Y., PEGORARO, E., NOBRE, A.D., PEREIRA, M.G.P., GRACE, J., CULF, A.D. and CLEMENT, R., 2002, Energy and water dynamics of a central Amazonian rain forest. *Journal of Geophysical Research-Atmospheres*, **107**, 8061, doi:10.1029/2001JD000623.

MALHI, Y. and WRIGHT, J., 2004, Spatial patterns and recent trends in the climate of tropical rainforest regions. *Philosophical Transactions of the Royal Society of London. Series B*, **359**, pp. 311–329.

MARENGO, J.A., NOBRE, C.A., TOMASELLA, J., OYAMA, M.D., DE OLIVEIRA G.S., DE OLIVEIRA R., CAMARGO, H., ALVES, L.M. and BROWN, I.F., 2008, The drought of Amazonia in 2005. *Journal of Climate*, **21**, pp. 495–516.

MCKEE, T.B., DOESKEN, N.J. and KLIEST, J., 1993, The relationship of drought frequency and duration to time scales. In *Eighth Conference on Applied Climatology*, 17–22 January 1993, Anaheim, CA, pp. 179–184 (Boston: Meteorological Society).

MCPHADEN, M., 2004, Evolution of the 2002/03 El Niño. *Bulletin of the American Meteorological Society*, **85**, pp. 677–695.

MIURA, T., HUETE, A.R., VAN LEEUWEN, W.J.D. and DIDAN, K., 1998, Vegetation detection through smoke-filled AVIRIS images: an assessment using MODIS band passes. *Journal of Geophysical Research*, **103**, pp. 32001–32011.

MIURA, T., HUETE, A.R., YOSHIOKA, H. and HOLBEN, B.N., 2001, An error and sensitivity analysis of atmospheric resistant vegetation indices derived from dark target-based atmospheric correction. *Remote Sensing of Environment*, **78**, pp. 284–298.

MONTEITH, J.L., 1973, *Principles of Environmental Physics* (London: Edward Arnold).

MONTEITH, J.L., 1981, Evaporation and surface temperature. *Quarterly Journal of the Royal Meteorological Society*, **107**, pp. 1–27.

MONTEITH, J.L., 1995, Accommodation between transpiration vegetation and convective boundary layer. *Journal of Hydrology*, **166**, pp. 251–263.

MORAN, M.S., JACKSON, R.D., RAYMOND, L.H., GAY, L.W. and SLATER, P.N., 1989, Mapping surface energy balance components by combining Landsat Thematic Mapper and ground-based meteorological data. *Remote Sensing of Environment*, **30**, pp. 77–87.

MYNENI, R.B., YANG, W., NEMANI, R., HUETE, A., DICKINSON, R., KNYAZIKHIN, Y., DIDAN, K., FU, R., NEGRÓN JUÁREZ, R., SAATCHI, S., HASHIMOTO, H., ICHII, K., SHABANOV, N., TAN, B., RATANA, P., PRIVETTE, J., MORISETTE, J., VERMOTE, E., ROY, D., WOLFE, R., FRIEDL, M., RUNNING, S., VOTAVA, P., EL-SALEOUS, N., DEVADIGA, S., SU, Y. and SALOMONSON, V., 2007, Large seasonal swings in leaf area of Amazon rainforests. *Proceedings of the National Academy of Sciences*, **104**, pp. 4820–4823.

NAGLER, P.L., CLEVERLY, J., GLENN, E., LAMPKIN, D., HUETE, A. and WAN, Z., 2005, Predicting riparian evapotranspiration from MODIS vegetation indices and meteorological data. *Remote Sensing of Environment*, **94**, pp. 17–30.

NEGRÓN JUÁREZ, R.I., HODNETT, M.G., FU, R., GOULDEN, M.L. and VON RANDOW, C., 2007, Control of dry season evapotranspiration over Amazonian forest as inferred from observations at a southern Amazon forest site. *Journal of Climate*, **20**, pp. 2827–2839.

NEGRÓN JUÁREZ, R.I., LI, W., FU, R., FERNANDES, K. and CARDOSO, A.O., 2008, Comparison of precipitation datasets over the tropical South American and African continents. *Journal of Hydrometeorology* (in review).

NEPSTAD, D.C., DE CARVALHO C.R., DAVISON, E.A., JIPP, P.H., LEFEBVRE, P.A., NEGREIROS, G.H., DA SILVA E.D., STONE, T.A., TREMBORE, S.E. and VIEIRA, S., 1994, The role of deep roots in the hydrological and carbon cycles of Amazonian forests and pastures. *Nature*, **372**, pp. 666–669.

NEPSTAD, D.C., LEFEBVRE, P., DA SILVA, U.L., TOMASELLA, J., SCHLESINGER, P., SOLORZANO, L., MOUTINHO, P., RAY, D. and BENITO, J.G., 2004, Amazon drought and its implications for forest flammability and tree growth: a basin-wide analysis. *Global Change Biology*, **10**, pp. 704–717.

Nepstad, D.C., Moutinho, P., Dias, M.B., Davidson, E., Cardinot, G., Markewitz, D., Figueredo, R., Vianna, N., Chambers, J., Ray, D., Guerreiros, J.B., Lefebvre, P., Sternberg, L., Moreira, M., Barros, L., Ishida, F.Y., Tohlver, I., Belk, E., Kalif, K. and Schwalbe, K., 2002, The effects of partial through fall exclusion on canopy processes, aboveground production, and biogeochemistry of an Amazon forest. *Journal of Geophysics Research*, **107**, 8085, doi:10.1029/2001JD000360.

Nishida, K., Nemani, R.R., Glassy, J.M. and Running, S.W., 2003b, Development of an evapotranspiration index from Aqua/Modis for monitoring surface moisture status. *IEEE Transactions on Geoscience and Remote Sensing*, **41**, pp. 493–501.

Nishida, K., Nemani, R.R., Running, S.W. and Glassy, J.M., 2003a, An operational remote sensing algorithm of land surface evaporation. *Journal of Geophysical Research*, **108**, 4270, doi:10.1029/2002JD002062.

Oliveira, R.S., Dawson, T.E., Burgess, S.S.O. and Nepstad, D.C., 2005, Hydraulic redistribution in three Amazonian trees. *Oecologia*, **145**, pp. 354–363.

Oliver, M.A. and Webster, R., 1990, Kriging: a method of interpolation for geographical information system. *International Journal of Geographical Information Systems*, **4**, pp. 313–332.

Potter, C., Davidson, E., Nepstad, D. and de Carvalho C.R., 2001, Ecosystem modeling and dynamic effects of deforestation on trace gas fluxes in Amazon tropical forest. *Forest Ecology and Management*, **152**, pp. 97–117.

Priante, N., Vourlitis, G., Hayashi, M., Nogueira, J., Campelo, J., Nunes, P., Souza, L., Couto, E., Hoeger, W., Raiter, F., Trienweiler, J., Miranda, E., Priante, P., Fritzen, C., Lacerda, M., Pereira, L., Biudes, M., Suli, G., Shiraiwa, S., Do Paulo, S. and Silveira, M., 2004, Comparison of the mass and energy exchange of a pasture and a mature transitional tropical forest of the southern Amazon Basin during a seasonal transition. *Global Change Biology*, **10**, pp. 863–876.

Priestley, C.H.B. and Taylor, R.J., 1972, On the assessment of surface heat flux and evaporation using large-scale parameters. *Monthly Weather Review*, **100**, pp. 81–92.

Salati, E., 1987, The forest and the hydrological cycle. In *The Geophysiology of Amazonia: Vegetation and Climate Interactions*, R.E. Dickinson (Ed.), pp. 273–296 (New York: John Wiley & Sons).

Sellers, P.J., Randall, D.A., Collats, G.J., Berry, J.A., Field, C.B., Dazlich, D.A., Zhang, C., Collelo, G.D. and Bounoua, L., 1996, A revised land surface parameterization (SiB2) for atmospheric GCMs, Part I: Model formulation. *Journal of Climate*, **9**, pp. 676–705.

Shein, K.A. (Ed.), 2006, State of the climate in 2005. *Bulletin of the American Meteorological Society*, **87**, pp. S1–S102.

Shuttleworth, W.J., 1988, Evaporation from Amazonian rainforest. *Proceedings of the Royal Society of London, Series B. Biological Sciences*, **233**, pp. 321–346.

Sombroek, W., 2001, Spatial and temporal patterns of Amazon rainfall. *Ambio*, **30**, pp. 388–396.

Sommer, R., Sa, T.D.D., Vielhauer, K., de Araujo A.C., Folster, H. and Vlek, P.L.G., 2002, Transpiration and canopy conductance of secondary vegetation in the eastern Amazon. *Agricultural and Forest Meteorology*, **112**, pp. 103–121.

Souza Filho, J.D., Ribeiro, A., Costa, M.H. and Cohen, J.C., 2005, Control mechanisms of the seasonal variation of transpiration in a northeast Amazonia tropical rainforest [in Portuguese]. *Acta Amazonica*, **35**, pp. 223–229.

Stokstad, E., 2005, Experimental drought predict grim future for rainforest. *Science*, **308**, pp. 346–347.

Su, H.B., McCabe, M.F., Word, E.F., Su, Z. and Prueger, J.H., 2005, Modeling evapotranspiration during SMACEX: comparing two approaches for local and regional scale prediction. *Journal of Hydrometeorology*, **6**, pp. 910–922.

VERMOTE, E.F., EL SALEOUS, N. and JUSTICE, C., 2002, Atmospheric correction of the MODIS data in the visible to middle infrared: first results. *Remote Sensing of Environment*, **83**, pp. 97–111.

VON RANDOW, C., MANZI, B., KRUIJT, A.O., DE OLIVEIRA P.J., ZANCHI, F.B., SILVA, R.L., HODNETT, M.G., GASH, J.H.C., ELBERS, J.A., WATERLOO, M.J., CARDOSO, F.L. and KABAT, P., 2004, Comparative measurements and seasonal variations in energy and carbon exchange over forest and pasture in South West Amazonia. *Theoretical and Applied Climatology*, **78**, pp. 5–26.

VOURLITIS, G.L., PRIANTE, N., HAYASHI, M.M.S., NOGUEIRA, J.D., CASEIRO, F.T. and CAMPELO, J.H., 2002, Seasonal variations in the evapotranspiration of a transitional tropical forest of Mato Grosso, Brazil. *Water Resources Research*, **38**, 1094, doi:10.1029/2000WR000122.

WALTER, I.A., ALLEN, R.G., ELLIOTT, R., JENSEN, M.E., ITENFISU, D., MECHAM, B., HOWELL, T.A., SNYDER, R., BROWN, P., ECHINGS, S., SPOFFORD, T., HATTENDORF, M., CUENCA, R.H., WRIGHT, J.L. and MARTIN, D., 2000, ASCE's standardized reference evapotranspiration equation. In *Proceedings 4th Decennial National Irrigation Symposium*, R.G. Evans, B.I. Benham and T.P. Trooien (Eds), pp. 209–215 (St Joseph, MI: American Society of Agricultural Engineers).

XIAO, X., HAGEN, S., ZHANG, Q., KELLER, M. and MOORE, B., III, 2006, Detecting leaf phenology of seasonally moist tropical forest in South America with multi-temporal MODIS images. *Remote Sensing of Environment*, **103**, pp. 465–473.

YANG, F., WHITE, M.A., MICHAELIS, A.R., ICHII, K., HASHIMOTO, H., VOTAVA, P., ZHU, A.-X. and NEMANI, R.R., 2006, Prediction of continental-scale evapotranspiration by combining MODIS and AmeriFlux data though support vector machine. *IEEE Transactions on Geosciences and Remote Sensing*, **44**, pp. 3452–3461.

ZHANG, Y., ROSSOW, W.B. and LACIS, A.A., 1995, Calculation of surface and top of atmosphere radiative fluxes from physical quantities based on ISCCP data sets. Part 1. Method and sensitivity to input data uncertainties. *Journal of Geophysical Research*, **100**, pp. 1149–1165.

ZHANG, Y., ROSSOW, W.B., LACIS, A.A., OINAS, V. and MISHCHENKO, M.I., 2004, Calculation of radiative fluxes from the surface to top of atmosphere based on ISCCP and other global data sets: refinements of the radiative transfer model and the input data. *Journal of Geophysical Research*, **109**, D19105, doi:10.1029/2003JD004457.